P1.15 ALONG-VALLEY STRUCTURE OF DAYTIME VALLEY FLOWS IN THE WIPPTAL

Magdalena Rucker[1*], Robert M. Banta[2] and Douw G. Steyn[1]
[1] The University of British Columbia, Vancouver, BC
[2] NOAA/Environmental Technology Laboratory, Boulder, CO

1. INTRODUCTION

Valley winds are local thermally-driven circulations that frequently form in valleys during undisturbed synoptic conditions. While previous research mainly focused on the mechanisms leading to the formation of valley flows and the temporal evolution of these flows, the spatial structure of valley flows, particularly in the along-valley direction, and the effects of local topography on valley flows remained relatively unexplored. This was partly due to the difficulty of obtaining detailed enough observations with traditional in-situ instrumentation. In more recent studies, the Doppler lidar has been successfully used to investigate fine-scale structures of nocturnal drainage flows (e.g. Post and Neff, 1986; Banta et. al., 1997).

During the Special Observing Period (SOP) of the Mesoscale Alpine Programme (MAP), a fair weather period provided the opportunity to study daytime valley flows in the Wipptal, Austria using the NOAA/ETL Doppler lidar. Observations which were obtained over several days showed day-to-day differences in the vertical structure of valley flow but similarities in the along-valley direction. In particular, an up-valley increase in wind speed was consistently observed. In this paper, we examine in detail the along-valley structure of daytime valley flows as observed on 17 October.

2. TERRAIN, INSTRUMENTATION AND SYNOPTIC CONDITIONS

The Wipptal is a predominantly NNW-SSE oriented valley that stretches 35 km from the Inntal, at the city of Innsbruck, south to the Brenner Pass. The valley floor has an average slope angle of 1.3^{o}. The portion of valley under study is a 12 km long section centered around the Doppler lidar site at Gedeir (Figure 1). A sharply rising ridgeline that separates the Wipptal from the tributary Stubaital forms a narrow and deep V-shaped valley in the vicinity of the lidar. Further up-valley, the Wipptal broadens somewhat before narrowing again at the terminus of the study area.

Several lidar scanning strategies were employed during this study. Vertical (RHI) scans along the center of the valley were performed to resolve the vertical structure of the along-valley flow. Due to a bend in the valley at Gedeir, azimuth angles of 178 and 320 degrees were used in the up- and down-valley direction, respectively (Figure 1). In addition, conical (VAD) scans at various elevation angles provided information on the cross-valley structure of the valley flow. The minimum range of the lidar varied between 1.2 and 1.5 km, while the maximum range (for this study) was roughly 6 km. The range gate resolution was 300 m. A more detailed description of the lidar can be found in Post and Cupp (1990).

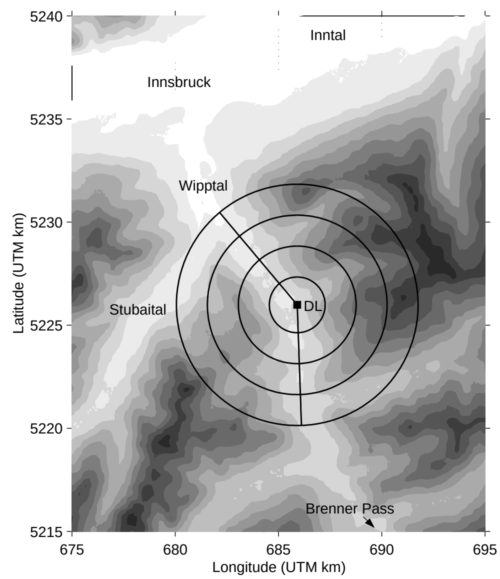

Figure 1: Location of Doppler lidar (DL) in the Wipptal. The straight lines mark RHI scans in the up- and down-valley direction. Circles indicate range gates at 1.35, 2.85, 4.35 and 5.85 km. Terrain contours are given at 200 m intervals, and terrain less than 600 m ASL is shown as white.

Measurements were obtained for five days during the period 11-17 October 1999. During this time, an upper level omega ridge positioned over central Europe provided dry, convective conditions over the Wipptal region. Synoptic flows varied somewhat with changes in strength and positioning of the blocking ridge, but were generally weak to moderate, and from the westerly to northerly direction. In the latter half of the study period, low lying clouds filled the Wipptal in the mornings, but dissipated by 1000 UTC. Diurnal valley flow characteristics were observed at most surface weather stations in the Inntal and Wipptal.

3. LIDAR MEASUREMENTS

Figure 2 shows the spatial structure of the along-valley flow at 1353 UTC on 17 October. The lidar

**Corresponding Author Address:* Magdalena Rucker, Atmospheric Science Program; Department of Earth and Ocean Sciences, The University of British Columbia, Vancouver, BC, V6T 1Z4; e-mail: rucker@geog.ubc.ca.

image represents an average of two consecutive RHI scan sequences, obtained within a 6-minute period. The valley flow which is roughly 800 m in depth is separated from the northwesterly flow aloft by a local minimum in wind speed. A RHI scan performed half an hour later (not shown here) displays a similar flow structure. In both RHI images, an up-valley increase in the along-valley flow component is visible. Figure 3 shows the along-valley volume flux density at 1353 and 1425 UTC. The volume flux density, defined as the ratio of volume flux and cross-sectional area (see Section 4), provides a measure of the mean velocity for the 800 m deep valley flow layer. Although no observations are available within the minimum range of the lidar, visual interpolation suggests that the along-valley increase in wind speed is most pronounced within a 1.5 - 2 km radius of the lidar where ridgelines on either side form a deep and narrow valley. Further up-valley, through the broader section of the valley, the wind speed still increases albeit at a lesser rate. It should be mentioned that the along-valley increase in wind speed - particularly through the narrow section of the valley - was observed on all study days under varying synoptic flows, although the magnitude in velocity increase varied in time and from day to day.

As the valley flow strengthens in the up-valley direction, the vertical flow structure changes as well (Figure 4). The lower velocity profiles down-valley from the lidar appear parabolic in shape, while the higher velocity profiles up-valley from the lidar show a closer correspondence to the Prandtl profile (Atkinson, 1981), with a distinct peak at about 200 m AGL.

From Figures 2 and 4, it appears that the flow above the effective ridgeline also accelerates in the up-valley direction. Since the flow above the valley is no longer restricted by valley sidewalls, the assumption of the RHI scans pointing along the flow

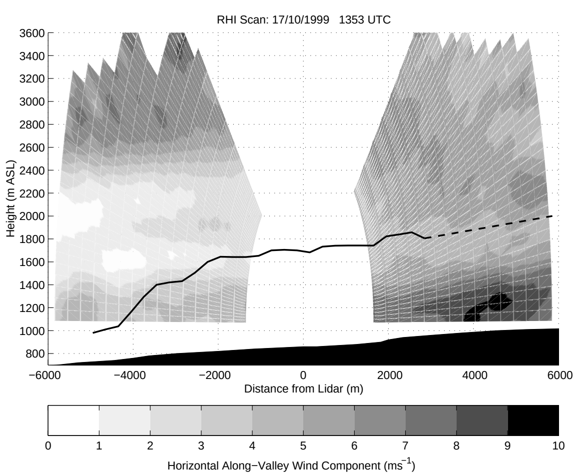

Figure 2: RHI images for 17 October at 1353 UTC, showing the horizontal along-valley flow component along the center of the Wipptal. Positive values indicate flow in the up-valley direction. Valley floor is shaded in black. The heavy solid/dashed line indicates the effective ridge height.

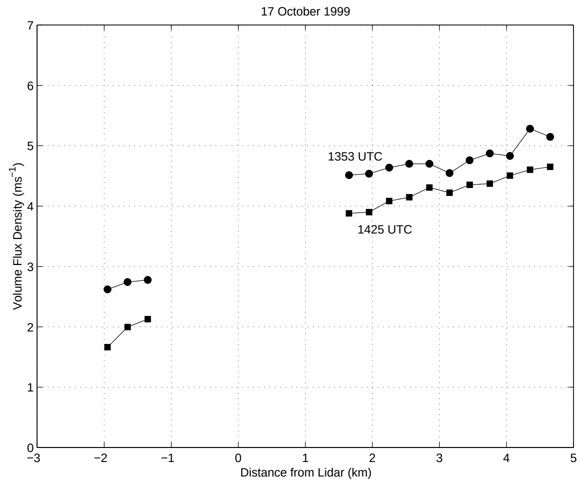

Figure 3: Along-valley volume flux density at 800 m AGL for 1353 UTC (circles) and 1425 UTC (squares) on 17 October.

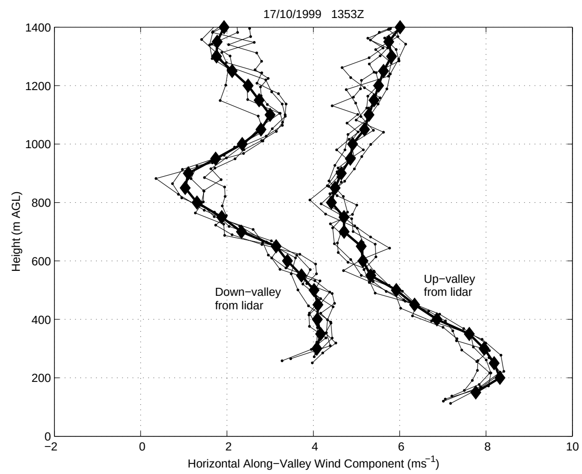

Figure 4: Vertical profiles of the horizontal along-valley wind component at 1353 UTC on October 17 for range gates 8-12 (2.25-3.45 km from lidar) both up- and down-valley from the lidar. Solid diamonds indicate averaged profiles.

direction may not hold true. To assess if the along-valley acceleration in the flow aloft is real or an artifact of the scanning strategy, VAD scans were analyzed for magnitude and direction of maximum radial velocity in the up- and down-valley direction. The analysis confirms that the flow velocity aloft increases in the along-valley direction up to a height of approximately 2600 m ASL.

4. VOLUME FLUX ANALYSIS

The volume flux at each range gate was calculated using the formula

$$V = F\sum_{i=1}^{n} A_i U_i$$

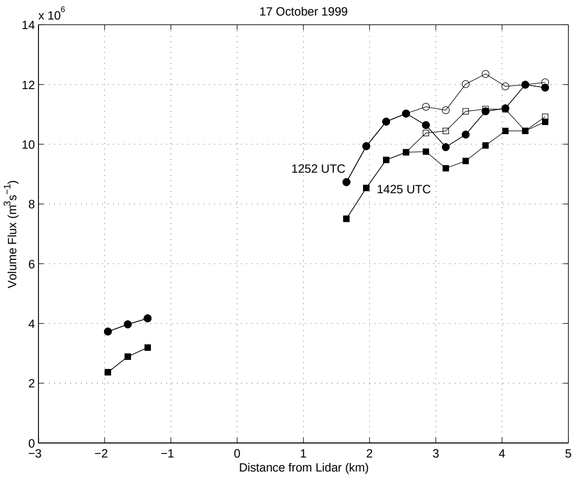

Figure 5: Along-valley volume flux at 800 m AGL for 1353 (circles) and 1425 UTC (squares) on 17 October. Open and solid symbols show the volume flux with and without tributary valleys, respectively.

where V is the volume flux, A_i is the cross-sectional area in the ith layer, U_i is the lidar-measured up-valley flow component of wind speed in that layer, and F equals the ratio of the mean up-valley flow component across the valley cross-section and U_i measured at the center of the valley. Analysis of cross-valley profiles from VAD scans for all study days provided an averaged value of 0.8 for F. Lidar derived wind profiles were linearly extrapolated to the valley floor, assuming zero wind speed at the surface. Cross-sectional areas for each range gate were determined from 100 m resolution digital topography data. Calculations of cross-sectional area were complicated by a number of small side valleys; estimations of cross-sectional areas were therefore made by including and excluding tributary valleys. Figure 5 which shows the along-valley volume flux at 1353 and 1425 UTC indicates that the volume flux generally increases in the up-valley direction. A comparison of the along-valley volume flux with volume flux density (Figure 3) suggests that the roughly two-fold increase in volume flux across the minimum range of the lidar (approximately 3 km in distance) is primarily due to the increase in along-valley flow component. Further up-valley from the lidar, the along-valley behavior of the volume flux is largely determined by along-valley variations in the cross-sectional area.

5. DISCUSSION

From the volume flux analysis, one can conclude that the along-valley velocity increase is not caused by a reduction in the valley cross-sectional area (i.e. mass conservation), but that the along-valley volume flux is diverging. By mass continuity, we expect subsidence to occur in this part of the valley. The persistent occurrence of the along-valley velocity increase suggests that it is linked with specific topographical features in this part of the Wipptal. One possible explanation for the up-valley acceleration is that an intra-valley pressure gradient develops in the narrow, deep section of the valley as a result of increased sensible heat input from the rising ridgeline. In a previous study, McKee and O'Neal (1989) showed that the intensity of drainage flows can be closely related to along-valley variations in valley geometry as defined by the volume effect or topographic amplification factor (TAF) (see Steinacker, 1984; Whiteman, 1990). A similar topographical analysis was completed for a 10 km section of the Wipptal whereby the TAF was calculated at each range gate for a 800 m deep layer. The analysis was performed twice, once with and once without tributary valleys. In both cases, the analysis did not show any significant along-valley changes in TAF, and therefore valley geometry – as defined by TAF - does not explain the occurrence of flow divergence in this part of the valley. It is questionable, however, if this analysis properly accounts for the effects of the rising ridgeline. The TAF analysis also does not take into account the sloping valley floor, or topographical features above the effective ridgeline (such as high-lying basins and mountain tops) which may contribute to the heating of air at greater heights. On most study days, an up-valley increase in wind speed was observed in the flow above the ridgeline. During morning transition periods, down-valley flow above the ridgeline ceased much earlier up-valley from the lidar than down-valley from the lidar. These observations suggest that differential heating occurred not only within the valley atmosphere, but also further aloft.

Observations of up-valley acceleration in daytime valley flows have also been reported by Freytag (1986) in the Inntal, and more recently by Egger et. al. (2000) in the Himalayan Kali Gandaki Valley. Both studies took place in valleys with terrain constrictions. Freytag (1986) hypothesizes that the increase in mass flux is due to quasi-local subsidence compensating for flow into tributary valleys. Observations in the Kali Gandaki Valley show that the valley flow accelerates through the terrain constriction, but also continues to accelerate in the widening part of the valley. Numerical modeling (Zängl et. al., 2001) suggests that the flow in the widening part of the valley resembles supercritical flow and appears to maintain its strength through inertia. It is unclear at this point if and how these two observations of volume flux divergence in daytime valley flows are related to observations in the Wipptal. Collectively, however, they suggest that volume flux divergence is not an uncommon occurrence in daytime valley flows.

6. SUMMARY

Doppler lidar observations made on several fair weather days during MAP-SOP documented the along-valley structure of daytime valley flows in the Wipptal. Although the vertical structure of the valley flow varied from day to day, an along-valley increase in wind speed through a narrow, deep section of the valley was observed on all study days. Analysis of the lidar data indicates that the volume flux diverges in the studied section of the Wipptal. The persistent occurrence of flow divergence in this part of the valley suggests that it is linked with specific topographical features. A TAF analysis, however, cannot explain the volume flux divergence in terms of along-valley changes in valley geometry.

Similar observations of along-valley volume flux divergence have been made in other valleys, but it is unclear if these flow divergences are caused by similar topographical features.

For future work, realistic and idealized numerical modeling will be used to investigate the relative importance of specific topographical features (such as valley geometry, sloping ridgelines, tributary valleys and high-lying terrain) on the along-valley structure of valley flows.

Acknowledgements. The authors wish to thank Georg Mayr for his organizational efforts of the MAP field campaign in the Brenner Pass area. Janet Intrieri, Richard Marchbanks and Lisa Darby provided valuable assistance in operating the lidar. Surface weather observations were kindly provided by Stephen Mobbs from the University of Leeds. The MAP deployment of the NOAA/ETL Doppler lidar was supported by NOAA/OAR. MR and DGS were partially funded by NSERC. NOAA/ETL provided partial travelling funds for MR.

REFERENCES

Atkinson, B.W., 1981: *Meso-scale Atmospheric Circulations*. Academic Press, 495 pp.

Banta, R.M., P.B. Shepson, J.W. Bottenheim, K.G. Anlauf, H.A. Wiebe, A. Gallant, T. Biesenthal, L.D. Olivier, C.-J. Zhu, I.G. McKendry and D.G. Steyn, 1997: Nocturnal cleansing flows in a tributary valley. Atmos. Env., **31**, 2147-2162.

Egger, J., S. Bajrachaya, U. Egger, R. Heinrich, J. Reuder, P. Shayka, H. Wendt and V. Wirth, 2000: Diurnal winds in the Himalayan Kali Gandaki Valley. Part I: Observations. *Mon. Wea. Rev.*, **128**, 1106-1122.

Freytag, C.,1986: Results from the MERKUR experiment: Mass budget and vertical motions in a large valley during mountain and valley wind. *Meteorol. Atmos. Phys*., **37**, 129-140.

McKee, T.B. and R.D. O'Neal (1989) The role of valley geometry and energy budget in the formation of nocturnal valley winds. *J. Appl. Meteor*., **28**, 445-456.

Post, M.J. and R.E. Cupp (1990) Optimizing a pulsed Doppler lidar. *Applied Optics*, **29**, 4145-4158.

Post,M.J. and W. Neff (1986) Doppler lidar measurements of winds in a narrow mountain valley. *BAMS*, **67**, 274-281.

Steinacker, R. (1984) Area-height distribution of a valley and its relation to the valley wind. *Beitr. Phys. Atmosph.*, **57**, 64-71.

Whiteman, C.D. (1990) Observations of thermally developed wind systems in mountainous terrain. In: Blumen, W. (ed), *Atmospheric Processes over Complex Terrain. Meteor. Monogr.*, **45**, 5-42.

Zängl, G., J. Egger and V. Wirth (2001) Diurnal winds in the Himalayan Kali Gandaki Valley. Part II: Modeling. *Mon. Wea. Rev.*,129,1062-1080.